Dielectric measurements during phase coexistence in DKDP crystals under rotating thermal gradient

1996 J. Phys.: Condens. Matter 8 11337

(http://iopscience.iop.org/0953-8984/8/50/054)

J. Phys.: Condens. Matter **8** (1996) 11337–11350. Printed in the UK

Dielectric measurements during phase coexistence in DKDP crystals under rotating thermal gradient

Jean Bornarel†, Ryszard Cach‡ and Zdenek Kvitek†

† Laboratoire de Spectrométrie Physique (UA CNRS No 8), Université Joseph Fourier BP 87, 38402 Saint-Martin-d'Hères, France

‡ Institute of Experimental Physics, University of Wroclaw, Pl. Maxa Borna 9, 50-205 Wroclaw, Poland

Received 8 May 1996, in final form 30 September 1996

Abstract. The dielectric properties of DKDP samples under a thermal gradient G_e are studied versus the orientation of G_e relative to the c ferroelectric axis. Simple models allow us to explain the variation of the dielectric constant in the paraelectric phase, and also demonstrate a contribution due to the phase front existence for the first time.

1. Introduction

At a temperature around 215 K, KD_2PO_4 (DKDP) crystals exhibit a first-order transtion between a tetragonal paraelectric phase, which is the high-temperature phase, and an orthorhombic ferroelectric and ferroelastic one. The DKDP transition has been studied by means of different techniques as recalled in a previous paper (Bornarel and Cach 1994). In the last few years the phase coexistence has been a centre of interest: synchrotron x-ray topographies (Aleshko-Ozhevskii 1992) and optical observations performed simultaneously with dielectric measurements allow a better knowledge of the phase front shapes and of the coexistence phenomena (Bornarel and Cach 1993, 1994). The great importance of an external thermal gradient has been demonstrated. When the external thermal gradient is parallel to the ferroelectric axis c, the phase front is quasiplanar near a (001) plane with a very regular motion during a paraelectric–ferroelectric (PF) transition cycle as well as during a ferroelectric–paraelectric (FP) one. The dielectric properties have been correlated with the phase front motion and with the domain texture existence. A model taking into account the thermal gradient in the sample allows us to calculate the contribution of the ferroelectric domains during the phase coexistence in the dielectric constant. In this particular configuration, with the c axis parallel to the external thermal gradient, the contribution of the phase front itself to the dielectric constant has not been demonstrated.

In a recent paper (Bornarel *et al* 1996), the effect of the angle α between the external thermal gradient G_e and the c axis on the phase front shapes has been reported. The first result concerns the phase front shape in the middle of the coexistence cycle, when paraelectric and ferroelectric regions exhibit the same volume. For α values lower than 60° (with $G_e = 0.2$ K mm^{-1}), the phase front is quasiplanar, making an angle β with the (001) plane lower than 22°. For greater α values the phase front trace in a (100) section appears with a zig-zag shape. In neither case does any part of the phase front make an angle greater than 25° with the (001) plane. The second result concerns the modification

0953-8984/96/5011337+14$19.50

of the phase front shape for a given α value in relation to its position in the sample: the effects of the sample boundaries, especially the corners, are important. For example, a phase front which is quasiplanar in the middle of the sample exhibits a zig-zag shape near the corners and β values are greater in these regions. A model where the sample is an ellipsoid with a different thermal conductivity from the surrounding medium allows us to calculate the isotherm position inside the sample and the ratio G_i/G_e versus the α angle (G_i is the internal thermal gradient in the model of the sample). The phase front positions, the result of the minimization of all the energies, and the isotherms are compared (Bornarel *et al* 1996).

The aim of the present paper is the following: to study the variation of the dielectric properties near the phase transition, especially during the phase coexistence, for DKDP crystals in a rotating thermal gradient and correlate these results with the observation of domains and phase fronts. The particular case $\alpha = 90^\circ$ is interesting because the phase front zig-zag shape remains relatively constant during a great part of the coexistence. Then a model will be proposed in the last section to explain the experimental results.

2. Experimental procedures

The experimental procedures have been already described in the previous papers (Bornarel and Cach 1994, Bornarel *et al* 1996). The DKDP crystals were grown by slow cooling of a supersaturated solution of KDP and heavy water. The weak tapering angle of the crystals (a few degrees of arc), room-temperature optical studies and the dielectric properties confirmed the good quality of the samples. The observed transition temperature corresponds to a deuteration concentration of 90% for the crystal used in the results in figures 2 and 3 (sample X) and of 83% for the crystal whose results are given in figure 4 and subsequent figures (sample Y). The samples were cut with a wire saw. The orientations of sample faces, which were tetragonal planes, were verified with x-ray Bragg diffraction (with accuracy of a minute of arc) and each face was polished on a wet silk cloth with an alcohol and heavy water solution. The sample dimensions are given in the text (results section). The sample is placed as shown in figure 1 in the helium gas exchange chamber of a cryostat, allowing optical observations in three perpendicular directions simultaneously with dielectric measurements. The angle α between the c axis of the DKDP sample and the vertical thermal gradient can vary between 0 and 90° with the (100) faces always in a vertical plane. The sample position is modified with the help of two copper wires glued on the c faces. These wires also play the role of electrical contacts on the semi-transparent gold electrodes evaporated on these faces. The sample capacitance and the dissipation factor measured with a HP 4274 A impedance meter allow us to calculate ε' and ε'' values with a relative accuracy of 3×10^{-3} and 10^{-2} respectively (with a measuring electric field of 1 V cm^{-1} in amplitude and 4 kHz in frequency). In the present paper the thermal gradient G_e remains constant and equal to 0.2 K mm^{-1} and the temperature may be regulated with an accuracy of a few millikelvins. The thermal treatment employed for runs is the following: in the temperature range of 3 K surrounding the phase coexistence region, continuous thermal temperature ramps (up and down) are performed by the regulator system. The cooling and heating rate is always lower than 10^{-2} K min^{-1}. Out of this temperature range stepwise heating and cooling is used with a $\frac{1}{2}$ h equilibration at each step. The temperature T indicated in the results section is measured by a platinum resistor placed near the glass window at the lowest part of the sample. The successive photographs during a transition cycle allow us to verify, as demonstrated in a previous paper (Bornarel *et al* 1996), that the repartition of the temperature can usually be deduced at a given point by the knowledge of T versus time.

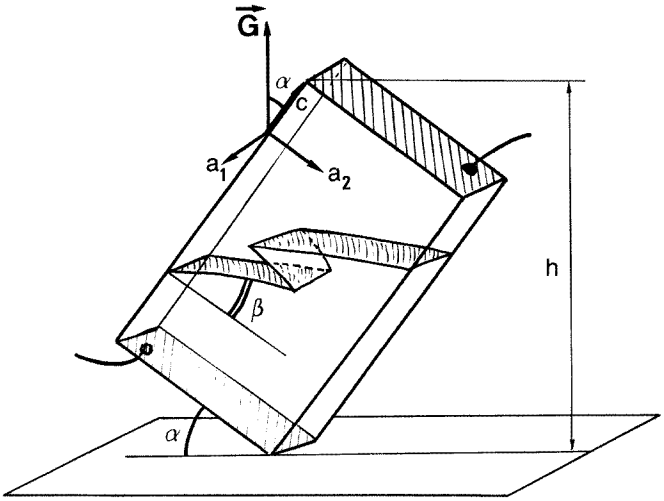

Figure 1. A schematic representation of a DKDP sample in a rotating thermal gradient G_e. The electrodes on the c faces are shown.

The internal thermal gradient G_i can also be calculated using this process. The phase front is continuously observed along the a_1 direction, which remains a horizontal axis, and the quality of the corresponding photographs is very good. The observations along the two other perpendicular directions (vertical and horizontal) are not so easy at every instant because of the refraction of the light on the sample boundaries. However it is always possible to rebuild the phase front shape and obtain information on the domain texture.

3. Results

Measurements of the dielectric constant ε_c' and of the loss constant ε_c'' along the c axis are performed simultaneously with observations of the domain texture and the phase front. It is decided to describe the case $\alpha = 90^\circ$ ($\boldsymbol{G}_e$ and $\boldsymbol{c}$ perpendicular) in detail and to underline which phenomena occur for all α values.

3.1. The paraelectric–ferroelectric cycle (PF)

Figure 2 illustrates the results obtained during a PF cycle with a sample X whose dimensions are $a_1 = 5.5$ mm, $a_2 = 4.4$ mm, $c = 7.4$ mm and with a deuteration equal to 90% ,under a thermal gradient G_e perpendicular to c. The internal thermal gradient magnitude is $G_i = 0.1$ K mm^{-1}. Figure 2(a) and (b) shows the $\varepsilon_c'^{-1}$ and ε_c'' variations as functions of the temperature T, and figure 2(c) shows photographs of the phase front trace in the a_1 direction. Different situations during the phase coexistence are indicated by capital letters, of which some are marked on the $\varepsilon_c'^{-1}(T)$ and $\varepsilon_c''(T)$ curves. For example A corrresponds to the appearance of phase front daggers on the lower a_2 sample face (the coolest ones). This face is in contact with the glass window with a conductivity similar to that of the DKDP crystal, and daggers are created in the centre of the face as well as in the corners (in B). Then the daggers overrun all the a_2 face. ε_c' increases slowly above the Curie–Weiss law and ε_c'' remains nearly constant during the beginning of this PF cycle. Between A and C no domains are observed by optical means, or with the help of a diffraction method

using a laser beam along the c axis (Hill and Ichiki 1964). In C the zig-zag shaped phase front leaves the a_2 sample face and the domains appear below the zig-zag phase front. Usually the domain walls are in a plane perpendicular to the thermal gradient, here in a (010) plane. The phase front moves without noticeable modification between C and E with simultaneous small fluctuations of ε_c' values and high variations of ε_c'' correlated to the domain wall rearrangements and the phase front displacement. In E the phase front reaches the upper a_2 sample face (the hottest one) in contact with the helium gas. The effect of the sample corners on the thermal repartition is well illustrated by photographs E–H. ε_c' changes smoothly, ε_c'' drastically when the daggers begin to move on the a_2 sample face and after that ε_c'' remains constant. In H all the sample volume is ferroelectric.

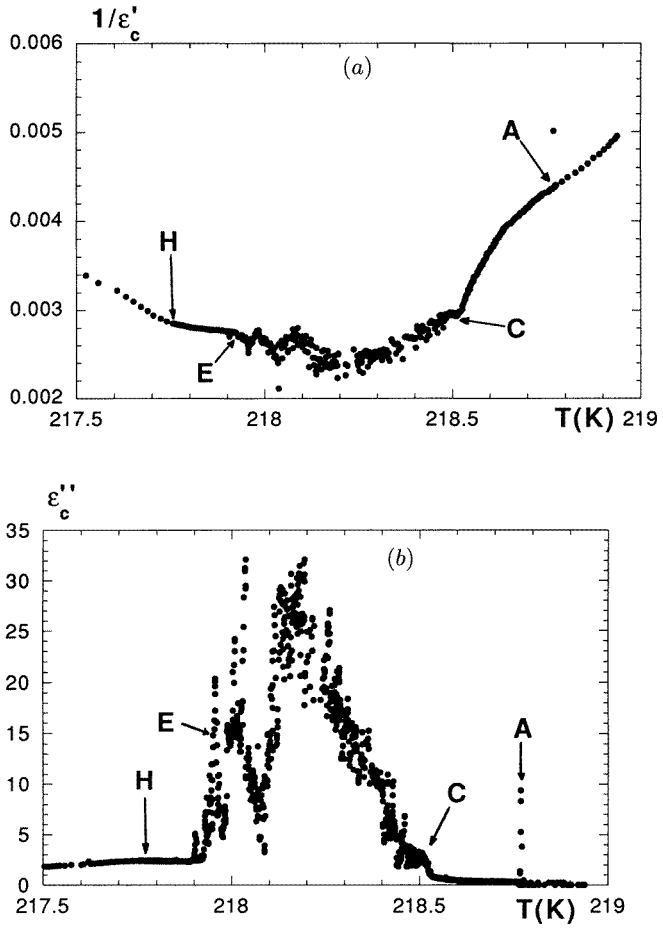

Figure 2. Results obtained during a PF transition for $\alpha = 90^\circ$ (sample X): (a) variation of the reciprocal values of the dielectric constant ε_c' versus the temperature T; (b) variation of the loss constant ε_c'' versus T; (c) photographs of the phase front along the a_1 direction.

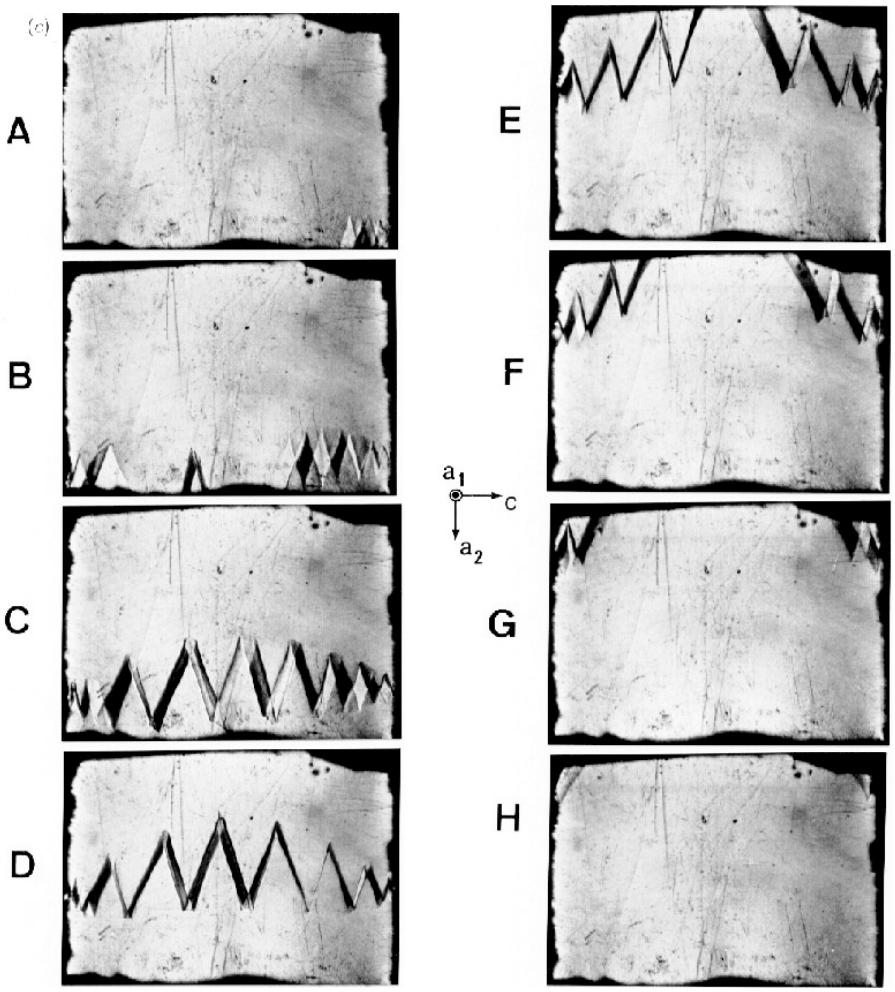

Figure 2. Continued.

3.2. The ferroelectric-paraelectric cycle (FP)

Figure 3 gives similar information to figure 2 obtained during an FP cycle. As already published, ε_c' and ε_c'' values are lower during an FP cycle than during a PF one: the domain texture has been stabilized by a period of 12 h in the ferroelectric phase. It seems that the increase of ε_c' and ε_c'' occurs before the appearance of the first nucleus of the paraelectric phase in A′, but it is difficult to optically detect very small nuclei. As during the PF cycle, ε_c' remains nearly constant and ε_c'' shows important modifications when the zig-zag phase front crosses the sample in the a_2 direction (between B′ and E′). Finally, during the translation and then the disappearance of the daggers on the lowest a_2 face, ε_c' is regularly modified, as well as ε_c'' (between E′ and F′). The domain texture does not change during the FP cycle, just scanned by the phase front.

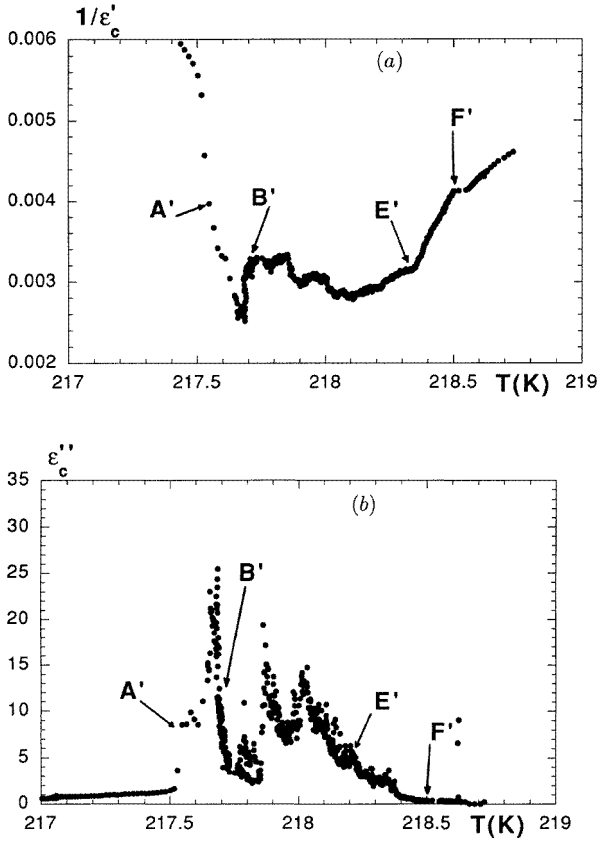

Figure 3. Dielectric measurements during an FP transition versus temperature for $\alpha = 90^\circ$: (*a*) $\varepsilon_c^{'-1}(T)$; (*b*) $\varepsilon_c''(T)$ (sample X). The paraelectric nuclei appear in A′ and the last ferroelectric nucleus disappears in F′. B′ and E′ correspond to separation of the zig-zag phase front from the a_2 sample boundaries.

3.3. The effect of the angle α on $\varepsilon_c'(T)$ and $\varepsilon_c''(T)$

PF and FP cycles were carried out with different α values and the following phenomena and results appear in all cases:

(i) the ferroelectric region inside the daggers appears as monodomain at the beginning of the PF cycles;

(ii) the domain arrangements always occur during the PF cycles and never during the FP ones, which explains the higher values of ε_c' and ε_c'' peaks for a phase front motion or a domain texture arrangement. Then $\varepsilon_c''(T)$ curves show their highest and most discontinuous values for α values between 60 and 90° (see figure 4(*b*)) because there are many possibilities for interactions among the daggers of the phase front, the domains and the sample boundaries, especially the corners. As for different cooling and heating cycles the accuracy of the absolute measured temperature T (at the lowest point of the sample) can change, the $\varepsilon_c^{'-1}$ and ε_c'' values are shown as functions of $T - T_1$ (T_1 is the temperature corresponding to the appearance of the ferroelectric nuclei at the beginning of a PF cycle). Figure 4(*a*) and (*b*) gives the $\varepsilon_c^{'-1}(T - T_1)$ and $\varepsilon_c''(T - T_1)$ curves respectively for PF

transitions. It is interesting to recall the different shapes of the phase front presented in a previous paper (Bornarel *et al* 1996): the phase front can be quasiplanar for lower values of the α angle, and always zig-zag shaped for $\alpha > 60^\circ$. In figure 4(a), the translation in temperature of the Curie–Weiss laws in the paraelectric phase when α changes is clearly observed, for the DKDP sample Y used ($a_1 = 2.41$ mm, $a_2 = 4.71$ mm, $c = 9.02$ mm; and deuteration equal to 83%). The temperature T_1 corresponds by hypothesis to the appearance of the ferroelectric nuclei on the lower a_2 sample face.

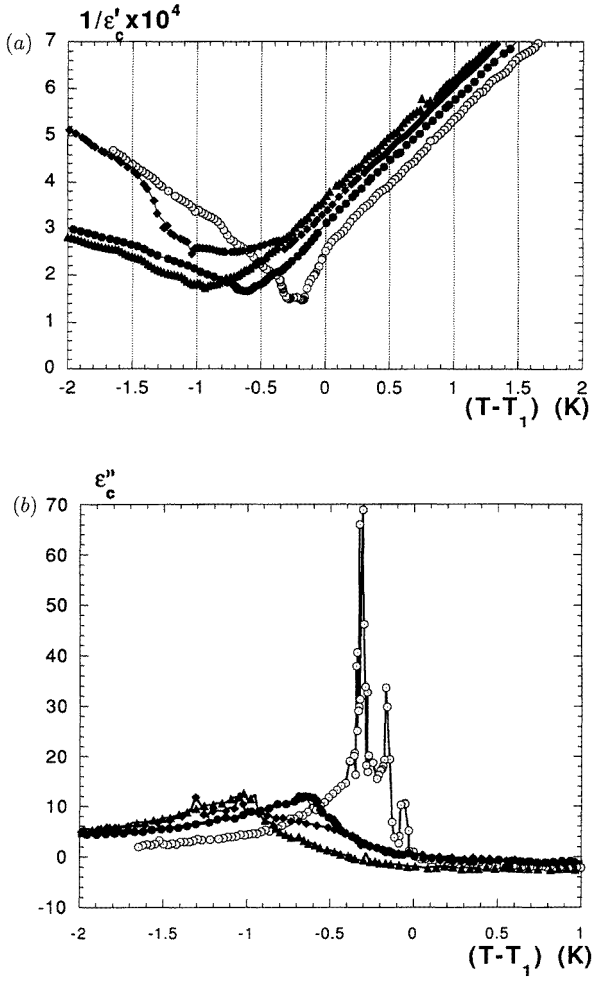

Figure 4. Variation of (a) $\varepsilon_c^{'-1}$ and (b) ε_c'' versus T during a PF cycle for different α values (sample Y): 90° (○), 69° (●), 23° (▲), and 0° (♦). The temperature T_1 corresponds to the appearance of the ferroelectric nuclei on the lower a_2 sample face.

If the curve $\varepsilon_c^{'-1}(T)$ for $\alpha = 0$ is taken as reference, a translation near low temperatures is observed when α increases up to 20° as shown by the curve T_0' versus α in figure 5(a) (within the paraelectric phase ε_c' varies as $(T - T_0')$. In contrast, when α increases above 40°, the value of T_0' becomes greater with an increasing α value. Another interesting result is given in figure 5(b), which shows the variation of $(T_1 - T_2)$ with the angle α value (T_2

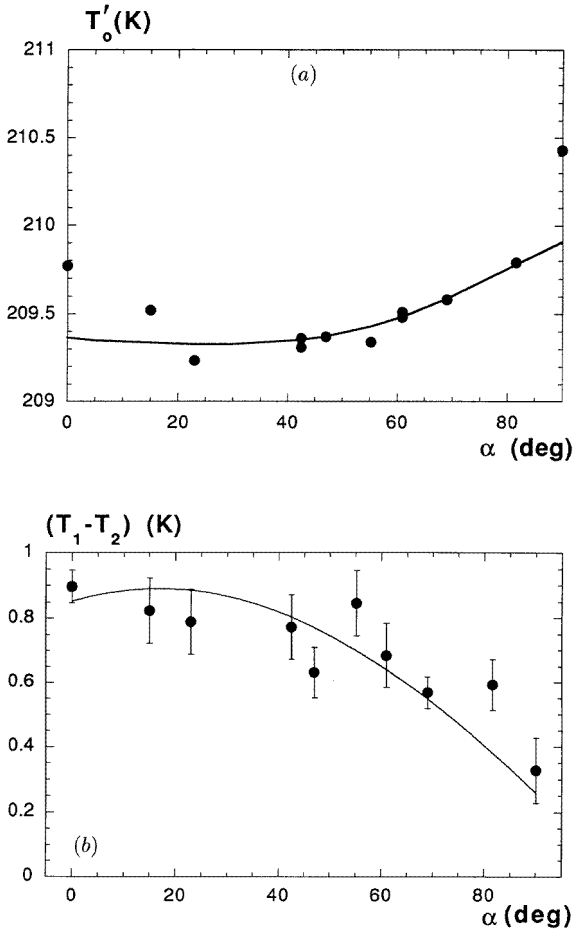

Figure 5. (*a*) Variation of the experimental value of T_0' with the andle α (PF cycles; $\varepsilon_c'^{-1}$ varies as $T - T_0'$ in the paraelectric phase; sample Y). (*b*) Variation of $(T_1 - T_2)$ with the angle α values in PF cycles. T_1 is the measured temperature of the beginning of the phase coexistence and T_2 corresponds to the end of the coexistence (sample Y).

corresponds to the end of the coexistence during a PF cycle). $(T_1 - T_2)$ is the temperature range where the phase coexistence exists and the variation shown in figure 5(*b*)is easily explained: if h_z is the sample dimension in the c direction, h_x that in the a_1 direction, and h the distance indicated in figure 1, $h = h_z \cos\alpha + h_x \sin\alpha$. With the hypothesis of a constant thermal gradient, $(T_1 - T_2)$ is calculated and the result corresponds to the continuous line in figure 5(*b*). The agreement with the experimental observations is relatively good taking the uncertainty of our measurements into account. Then, in a first approximation, it can be concluded that the variation of angle α does not change the G_e distribution too much.

4. Discussion

A result shown in the previous section concerns the translation in temperature of the paraelectric Curie–Weiss laws. This phenomenon is well known and explained for a sample under a thermal gradient parallel to the ferroelectric axis as follows.

The simplest thermodynamical potential (in a monodomain sample), for a first-order transition, can be written in terms of the relation

$$\Phi - \Phi_0 + (A/2)\big(T - T_0\big)P^2 - BP^4/4 + CP^6/6 + \dots \tag{1}$$

with P the polarization as order parameter and A, B, and C positive constants. The inverse of the dielectric susceptibility, approximated to $1/\varepsilon'_P$, follows a Curie–Weiss law for an isothermal sample in the paraelectric phase.

$$1/\varepsilon'_P = A\big(T - T_0\big). \tag{2}$$

If the sample is under a thermal gradient parallel to the c axis, it is easy to demonstrate that the measured dielectric constant can be written

$$1/\varepsilon'_P = A\big(T + \Delta T/2 - T_0\big). \tag{3}$$

T, as defined in the present paper, is the measured temperature at the lowest face of the sample and $\Delta T = G_e h_z$.

In the present paper, the sample rotates inside an external thermal gradient and the problem can be modelled as follows. Even if the differences between the thermal conductivities for the sample are neglected, conductivities between the paraelectric phase and the ferroelectric one, conductivities in the directions a or c, it is necessary to take into account the difference between the sample conductivity of the DKDP sample and that of the surrounding helium gas. A very simple model describes the sample as an ellipsoid which allows us to obtain a constant internal thermal gradient G_i (the corner effects are neglected). Then the magnitude of G_i is different from the G_e value:

$$G_i/G_e = \Big[\big(K_C \cos\alpha\big)^2 + \big(K_A \sin\alpha\big)^2\Big]^{1/2} \tag{4}$$

and also the orientation of G_i is not the same as that of G_e:

$$\beta = \tan^{-1}\big[K_A \tan\alpha/K_c\big] \tag{5}$$

with β the angle between the isotherms inside the sample and the (001) plane, and K_A and K_C parameters, functions of the conductivities (helium and the DKDP crystal) and of the sample shape.

The relations (4) and (5) demonstrated in a previous paper (Bornarel *et al* 1996), allow us to calculate the orientation and magnitude of the internal thermal gradient G_i in all the experimental cases reported here. With these very simple hypotheses, where G_i is considered the same throughout the sample, the temperature T' at a particular point (see figures 1 and 6) can be given versus T:

$$T'(z,\ x) = \boldsymbol{G}\cdot\boldsymbol{r} + T = G_i(z\cos\alpha + x\sin\alpha) + T. \tag{6}$$

The capacitance of the sample can be calculated as the combination of parallel capacitors (electrodes in (001) planes) each of which is the combination of capacitors in series. If the classical approximation for a plane capacitor is used, the measured macroscopic dielectric constant ε'_c can be finally obtained by

$$\varepsilon'_c = \frac{1}{h_x}\int_0^{h_x} \varepsilon'_P(x) \qquad \frac{h_x}{\varepsilon'_P(x)} = \int_0^{h_z} \frac{\mathrm{d}z}{\varepsilon'_P(z,\ x)} \tag{7}$$

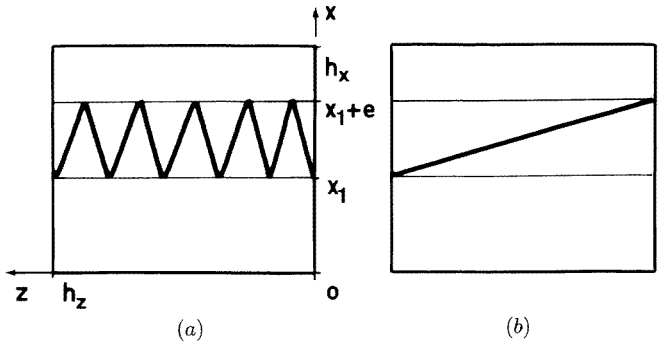

Figure 6. (*a*) A schematic representation of the phase front in the case $\alpha = 90^\circ$; (*b*) a theoretical scheme for calculation of the dielectric constant.

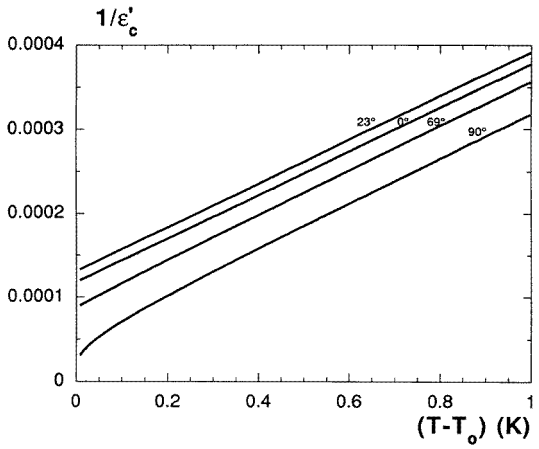

Figure 7. The calculated value of the reciprocal value of ε'_c in the paraelectric phase for different values of the β angle, versus $T - T_0$ (with $G_i = 0.16$ K mm^{-1}).

where $\varepsilon'_P(z, x)$ is the local value of the paraelectric dielectric constant and h_x and h_z the dimensions of the sample along a_2 and c as shown in figure 6.

Using (6) and (7), it is easy to obtain

$$\varepsilon'_P(T) = \frac{1}{AG_x h_x \sin\beta} \log\left[1 + \frac{G_i h_x \sin\beta}{T - T_0 + [(G_i \cos\beta)/2]h_z}\right]. \tag{8}$$

The relation (8) allows us to draw the curves $\varepsilon_c^{'-1}(T - T_0)$ shown in figure 7, using the values h_x and h_z, always the same value for G_e and also $A^{-1} = 3850$ K obtained with the experimental curve. There is a qualitative agreement between the experimental results in figure 4(*a*) and the calculated curves in figure 7. It is possible to note that the curves $\varepsilon_c^{'-1}(T)$ corresponding to the relation (8) look like straight lines, for $(T - T_0)$ greater than 0.1 K. However an important discrepancy exists as illustrated in figure 5(*a*) where the continuous line corresponds to the results of relation (8) (with $G_i = 0.16$ K mm^{-1}). The experimental values T'_0 at $\alpha = 0$ and $\alpha = 90^\circ$ are clearly higher than the calculated ones. This is because there are different experimental conditions between the cases $\alpha = 0$ and 90° where the

lowest face of the sample is in contact with a glass window with similar conductivity and the other α cases where only a corner touches this glass. It can be reasonably supposed that the thermal distributions in the lowest sample part differ in these two situations. The analysis is not simple because the conductivities but also the convection are to be taken into account. More accurate experiments are in progress in our group to study the thermal boundary conditions for the sample faces. They confirm the interest and the difficulty of the problem, especially when α values are between 20 and 80°. It is also in this α range that interactions between the phase front and the sample corners are stronger. Then, in the following, only the simple case $\alpha = 90°$ is studied and a model proposed for the dielectric constant.

First, it is necessary to recall that for an isothermal monodomain sample described by the relation (1) for its thermodynamical potential, the dielectric constant in the paraelectric phase ε'_P is given by the relation (2). If the transition is a first-order one, the dielectric constant of this monodomain sample in the ferroelectric phase ε'_F can be written as follows:

$$1/\varepsilon'_F = 4A\left(T^* - T\right) - \left(2A^{1/2}B/C^{1/2}\right)\left(T^* - T\right)^{1/2} \tag{9}$$

with the usual relation $T^* = T_0 + B^2/4AC$ where T^* is the limit of the phase coexistence range.

The Curie temperature, which corresponds to an equal value of the thermodynamical potential in both phases (paraelectric and ferroelectric) is

$$T_C = T_0 + 3B^2/16AC.$$

The situation described by the scheme 6(a) corresponds to a sample under a thermal gradient G_e with $\alpha = 90°$ and, in this case, the phase front during the coexistence has a zig-zag shape in an a_1 section.

The thermal gradient is considered as homogeneous in the whole sample and the problem is studied only in the (100) plane. Then, the temperature inside the crystal changes linearly with the position x:

$$T'(x) = T + \left(x/h_x\right)\Delta T \tag{10}$$

where ΔT is the difference between the temperature of the highest and the lowest a_2 faces of the sample, and is also equal to $T_2 - T_1$ because of the linear repartition of the temperature. The capacitance measured between the c electrodes is

$$C = \frac{1}{h_x}\int_0^{h_x} G(x)\,\mathrm{d}x.$$

It is possible to consider C as the sum of three contributions: one corresponds to the paraelectric region, another to the region of phase coexistence, and the last to the ferroelectric region. Then in the hypothesis where only the monodomain contribution is taken into account, the measured dielectric constant ε'_c can be written as follows:

$$\varepsilon'_{mono}(T) = \frac{1}{h_x}\left[\int_0^{x_1}\varepsilon'_F(x)\,\mathrm{d}x + \int_{x_1}^{x_1+e}\varepsilon'_{FP}(x)\,\mathrm{d}x + \int_{x_1+e}^{h_x}\varepsilon'_P(x)\,\mathrm{d}x\right]. \tag{11}$$

$\varepsilon'_P(T)$ and ε'_F terms correspond to the results of combinations of parallel capacitances, in the paraelectric phase and in the ferroelectric one respectively, and, using $\Delta T = T_2 - T_1 = h_x G_i$, it is easy to obtain

$$\varepsilon'_P(T) = (1/2A\,\Delta T)\,\log\left[\left(T + \Delta T - T_0\right)/\left(T - T_0\right)\right] \tag{12}$$

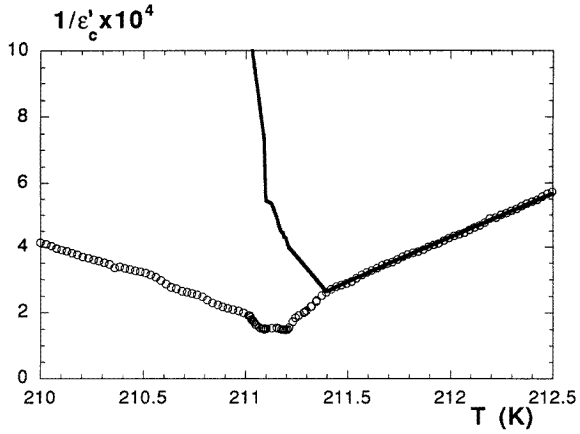

Figure 8. Variation of the reciprocal value of ε'_c versus T for $\alpha = 90°$. The white circles correspond to the dielectric measurements (samples Y) and the black line to the model of coexistence between two monodomain phases (ε'_{mono}).

and

$$\varepsilon'_F(T) = \frac{1}{2A\,\Delta T}\,\log\left[\frac{B + (B^2/4 + 4AC(T_C - T))^{1/2}}{B + (B^2/4 + 4AC(T_C - T - \Delta T))^{1/2}}\right]. \tag{13}$$

$\varepsilon'_{FP}(T)$ is the contribution to $\varepsilon'_c(T)$ corresponding to the phase coexistence region between the planes $x = x_1$ and $x = x_1 + e$. It can be noted that this contribution is the same as the one created by a quasiplanar phase front in the same volume as illustrated in figure 6(*b*). Then the second term of the relation (11) can be calculated by

$$h_x/\varepsilon'_{FP}(x) = z(x)/\varepsilon'_F(x) + \big[h_z - z(x)\big]/\varepsilon'_P(x)$$

and

$$\varepsilon'_{FP}(T) = \frac{1}{e}\int_{x_1}^{x_1+e} \varepsilon'_{FP}(x)\,\mathrm{d}x. \tag{14}$$

The term $\varepsilon'_{FP}(x)$ in the integral can also be written in function of T' as follows:

$$\frac{1}{\varepsilon'_{FP}}(T') = \frac{3B^2}{16C} + A\big(T' - T_c\big) + \frac{T'(x_1+e) - T'(x)}{T'(x_1+e) - T'(x_1)} \times\left[\frac{B^2}{16C} - 5A\big(T' - T_c\big) + \frac{B}{C}\left(\frac{B^2}{4} - 4AC\big(T' - T_c\big)\right)^{1/2}\right]. \tag{15}$$

If, by hypothesis, the isotherm $T' = T_c$ is taken to be in the middle of the phase coexistence region, using the value of $B = 4.5 \times 10^{10}$ SI previously estimated (Sidnenko and Gladkii 1973) and our observed values for T_0, T_c and ΔT, it is possible to calculate numerically $\varepsilon'_{FP}(T)$ and then $\varepsilon'_{mono}(T)$ as given by the relation (11). Figure 8 shows the experimental results for $\varepsilon'_c(T)$ and the calculated value using relations (12)–(14).

To explain the difference between the two curves, it is necessary to recall that the dielectric constant can be described as the sum of three contributions:

$$\varepsilon'_c = \varepsilon'_{mono} + \varepsilon'_f + \varepsilon'_d. \tag{16}$$

ε'_{mono} is the contribution previously calculated corresponding to a sample monodomain in both phases; ε'_f the contribution due to the phase front existence; and ε'_d the contributions

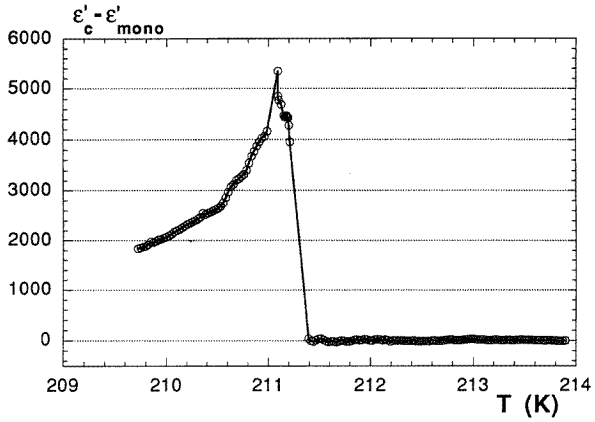

Figure 9. Variation of $\varepsilon'_c - \varepsilon'_{mono}$ versus T ($\alpha = 90°$; sample Y).

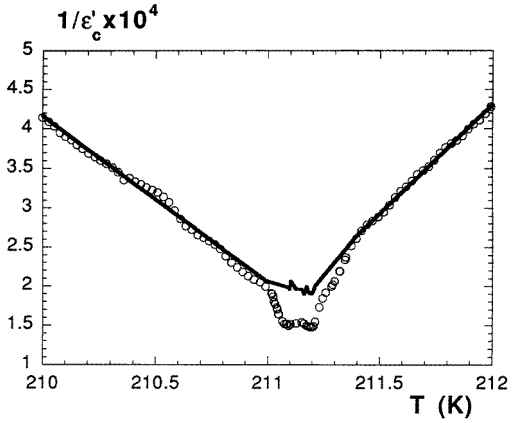

Figure 10. Reciprocal dielectric constant ε'_c versus T. The black line corresponds to the model but the variation in the ferroelectric phase has been approximated by a law $M'/T'_2 - T(\alpha = 90°)$.

of the domains. It is easy to calculate the difference $(\varepsilon'_c - \varepsilon'_{mono})$ between the measured dielectric constant and the contribution previously calculated. $(\varepsilon'_c - \varepsilon'_{mono})$ is depicted in figure 9. If the very sharp jump observed at the beginning of the PF cycle is an open problem, in contrast, the contribution of the domains to the dielectric constant is well known in the KDP family crystals (Barkla and Finlayson 1953, Bornarel 1987). This contribution in the ferroelectric phase, far from the transition, is several orders of magnitude greater than the monodomain ones and can be experimentally estimated by

$$\varepsilon'_{mono}(T) + \varepsilon'_d(t) = M'/\left(T'_2 - T\right) \tag{17}$$

with $M' = 4372$ K and $T'_2 = 211.85$ K .

Using the relations (11), (16), and (17), a calculated value of $\varepsilon'_{mono} + \varepsilon'_d$ can be obtained for each temperature. It corresponds to the continuous line in the representation $(\varepsilon'_c)^{-1}$ versus T given in figure 10. The agreement between this curve and the experimental results is very good in the ferroelectric and paraelectric phases, but the measured dielectric constant appears greater during the phase coexistence. The difference between the measured

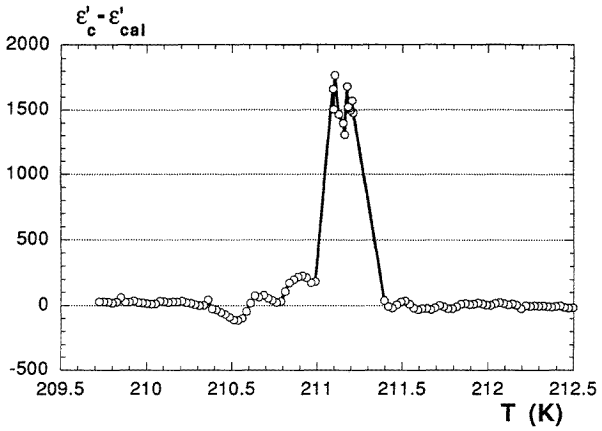

Figure 11. $\varepsilon'_c - \varepsilon'_{calc}$ versus T: contribution to the dielectric constant which can be attributed to the phase front ($\alpha = 90°$).

dielectric constant ε'_c and the calculated $\varepsilon'_{calc} = \varepsilon'_{mono} + \varepsilon'_d$, reported in figure 11, can be attributed to a phase front contribution ε'_f. As a precaution, it is better to affirm that this contribution is directly related to the existence of the phase front. It is evident that the samples studied are shaped so that the evaluation of the permittivity even in zero gradient, requires a non-trivial formula that incorporates the edge correction, which increases with increasing sample dimension in the c direction. Moreover the sample dielectric constant plays an important role. Then, if the purpose were to study the quantitative variation of ε'_f, using a trivial formula would not be sufficient. However the fact that using these formula allows us to obtain $\varepsilon'_c - \varepsilon'_{cal}$ equal to zero out of the phase coexistence region shows that this approximation is correct in the context because of the high value of the dielectric constant (between 1000 and 10 000). Experiments are in progress in our laboratory to correlate the dielectric constant and the loss constant variations with the volume of the phases and with the surface value of the phase front. The first results are encouraging.

To conclude, the dielectric properties of a DKDP sample under a thermal gradient (typically equal to 10^{-1} K mm^{-1}) change very much with the relative orientation of the thermal gradient and the crystallographic axes of the crystal, expecially the c one. A very simple model for the temperature distribution inside the sample is sufficient to explain the variation of the dielectric constant in the paraelectric phase. The models used to calculate the dielectric constant demonstrate that, during the phase coexistence, a contribution due to the phase front exists in addition to the monodomain (ferroelectric and paraelectric) ones and to that due to the domains.

References

Aleshko-Ozhevskii O P 1992 *Sov. Phys.–Solid State* **34** 499
Barkla H M and Finlayson D M 1953 *Phil. Mag.* **44** 109
Bornarel J 1987 *Ferroelectrics* **71** 255
Bornarel J and Cach R 1993 *J. Phys.: Condens. Matter* **5** 2977
——1994 *J. Phys.: Condens. Matter* **6** 1663
Bornarel J, Cach R and Kvitek Z 1996 *J. Phys.: Condens. Matter* **8** 7377
Hill R M and Ichiki S K 1964 *Phys. Rev.* **135** A1640
Sidnenko E V and Gladkii V V 1973 *Sov. Phys.–Crystallogr.* **17** 861